Cerebral Cortex January 2015;25:147–160
doi:10.1093/cercor/bht214
Advance Access publication August 19, 2013

Systematic, Cross-Cortex Variation in Neuron Numbers in Rodents and Primates

Christine J. Charvet[1], Diarmuid J. Cahalane[2] and Barbara L. Finlay[1]

[1]Behavioral and Evolutionary Neuroscience Group, Department of Psychology and [2]Center for Applied Mathematics, Cornell University, Ithaca, NY 14853, USA

Address correspondence to Christine J Charvet, 229 Uris Hall, Psychology, Cornell University, Ithaca, NY 14853-7601, USA. Email: cjc337@cornell.edu

Uniformity, local variability, and systematic variation in neuron numbers per unit of cortical surface area across species and cortical areas have been claimed to characterize the isocortex. Resolving these claims has been difficult, because species, techniques, and cortical areas vary across studies. We present a stereological assessment of neuron numbers in layers II–IV and V–VI per unit of cortical surface area across the isocortex in rodents (hamster, *Mesocricetus auratus*; agouti, *Dasyprocta azarae*; paca, *Cuniculus paca*) and primates (owl monkey, *Aotus trivigratus*; tamarin, *Saguinus midas*; capuchin, *Cebus apella*); these chosen to vary systematically in cortical size. The contributions of species, cortical areas, and techniques (stereology, "isotropic fractionator") to neuron estimates were assessed. Neurons per unit of cortical surface area increase across the rostro-caudal (RC) axis in primates (varying by a factor of 1.64–2.13 across the rostral and caudal poles) but less in rodents (varying by a factor of 1.15–1.54). Layer II–IV neurons account for most of this variation. When integrated into the context of species variation, and this RC gradient in neuron numbers, conflicts between studies can be accounted for. The RC variation in isocortical neurons in adulthood mirrors the gradients in neurogenesis duration in development.

Keywords: cortex, development, gradient, numbers

Introduction

Though the fundamental structure of the isocortex has been the object of intense study for over a 100 years, whether a basic feature of its organization, the number of neuron numbers per "cortical column," is constant or variable across species and cortical areas has remained a point of controversy. A widely cited study by Rockel et al. (1980) concluded that neuron numbers under a unit of cortical surface are constant across the isocortex with the exception of the primary visual cortex (V1), which had many more neurons than other areas. The work of Rockel et al. (1980) has been disputed for its lack of stereological techniques, relatively few samples through the isocortex and a limited range of species (Rakic 2008). Although numerous other studies have demonstrated within-species variation in neuron numbers per unit of cortical surface area (O'Kusky and Colonnier 1982; Finlay and Slattery 1983; Beaulieu and Colonnier 1989; Finlay 1992; Hutsler et al. 2005; Sherwood et al. 2007; Collins et al. 2010; Campi et al. 2011; Collins 2011; Cahalane et al. 2012; Lewitus et al. 2012; Young et al. 2013) the idea that neuron numbers under a unit of cortical surface area is uniform across the isocortex has persisted (Carlo and Stevens 2013).

As Rakic (2008) notes, the varying definitions of a cortical column across studies are one of the principle problems. In addition, the techniques used to estimate neuronal numbers have varied from uncorrected counting from sectioned material, "assumption-based" stereology, "assumption-free" stereology (optical fractionator), and more recently the isotropic fractionator, where labeled, dissociated cells are counted by microscopy. Further limiting the scope of available data, the species chosen for study have been in large part the standard laboratory animals and the most commonly selected areas are the primary sensory and motor areas. Most recently, Carlo and Stevens (2013) used standard stereological methods to replicate and confirm the study by Rockel et al. (1980). However, just as in the study reported by Rockel et al. (1980), these authors restricted their analyses to a few cortical areas without systematically sampling the frontal to caudal poles of the isocortex. Similarly, the authors restricted their analyses to a few species (i.e., mouse, rat, cat, rhesus monkey). It is therefore not clear whether neuron numbers vary systematically across the rostro-caudal (RC) axis of the isocortex and across species.

Recently, the isotropic fractionator method has been used as an alternative to standard stereological techniques. Previous reports (Herculano-Houzel and Lent 2005; Collins et al. 2010) examined the whole volumes of brain regions designated as the cerebral cortex and cerebellum. Neurons and glia in a given brain region were homogenized and then counted. Collins et al. (2010) used the isotropic fractionator method to estimate neuron numbers in smaller regions across the isocortex of 4 primate species. This study showed that cortical areas vary greatly (up to 5 times) in neuronal densities and neuron numbers per unit of cortical surface area within and across species. In a further analysis of these primate data in addition to data collected in 3 other primate species, we characterized a pronounced RC gradient in neuron numbers per unit of surface area across the isocortex (Cahalane et al. 2012). Neuron numbers per unit of cortical surface area are lowest in the frontal cortex, rising steadily toward the occipital or caudal pole (i.e., V1). Overlaid on this gradient, primary sensory areas exhibit elevated numbers per unit of cortical surface area.

As a method to understand the comparative and developmental structure of species differences in cortical organization, the isotropic fractionator method is limited, as only relative large volumes of tissue can be dissected from fresh brains, identification of areal boundaries is difficult in gross dissection, and features such as cortical layers and neuron types are inaccessible. We have therefore estimated neuron numbers per unit of cortical surface area in sectioned material, using stereological techniques, to systematically investigate neuron numbers across the isocortical surface of rodent and primate brains that vary widely in volume. One focus of this study is the identification of the laminar contributions to differences in neuron numbers across the isocortex. We also analyzed the systematic relationships between cortical volume, surface area, number of neurons per unit surface area, and position across

the cortical surface. We also compare neuron number estimates assessed with the use of standard stereological techniques and the isotropic fractionator method to identify potential sources of consistency and variability in the hope of resolving persisting controversies.

Our stereological analysis departs from the traditional approach, which has been to estimate neuron numbers in select cortical areas (Rockel et al. 1980; O'Kusky and Colonnier 1982; Beaulieu and Colonnier 1989; Finlay 1992; Sherwood et al. 2007; Collins et al. 2010; Lewitus et al. 2012; Carlo and Stevens 2013) in that we systematically sampled sites across the RC and medio-lateral (ML) axes of the isocortical sheet, choosing a set of species in which the size of the isocortical sheet varies relatively systematically. We hypothesized that the RC gradient in neurogenesis timing (Bayer and Altman 1990, 1991; Rakic 2002) during development, whereby the comparatively longer duration of neurogenesis in caudal regions may lead to greater neuron numbers in those regions, is the source of systematic variation in neuron numbers across the isocortex in adulthood. We therefore focused on the axes of the isocortical sheet rather than select cortical areas.

We found a rostral-caudal gradient in neuron numbers under a unit of cortical surface, which accounts for a significant percentage of the variance across the isocortex. The gradient in neuron numbers is more pronounced in primates than in rodents and the range of variation in neuron numbers across the isocortex is more pronounced in species with large isocortices. Furthermore, the variation in total neuron numbers under a unit of cortical surface area is principally due to variations in supragranular (II–IV) layer neuron numbers while the number of infragranular neurons varies less across the isocortex.

Materials and Methods

The first consideration in choice of species was variation in brain size. To that end, we selected brains that vary by a factor of 6 in monkeys and by a factor of 30 in rodents. Three species of New World monkeys (1 golden-handed tamarin, *Saguinus midas*; 1 northern owl monkey, *Aotus trivirgatus*; 1 black howler monkey, *Cebus apella*; and 3 rodent species (1 hamster, *Mesocricetus auratus*; 1 agouti, *Dasyprocta azarae*; 1 paca, *Cuniculus paca*) were used. For the choice of specimen, each brain's processing had to permit stereological assessment of neuron number and reconstruction of cortical curvature.

Initial perfusions used 4% paraformaldehyde. One to two weeks later, the brains were stored in a 2% paraformaldehyde solution. The brains were placed in 30% sucrose and then sectioned coronally on a freezing microtome. The sections were stained with cresyl violet. The brain weight, section thickness and specimen ID are listed in Table 1. The animals were treated in compliance with the principles defined by the National Institutes of Health Guide for the Care and Use of Laboratory Animals, as certified by Cornell University's Institutional Animal Care and Use Committee. These specimens were used in previous studies (Kaskan et al. 2005; Chalfin et al. 2007; Cahalane et al. 2012).

Optical Fractionator Method

Sections were examined with a Leitz Diaplan microscope and a Neurolucida imaging system with a mechanical stage (Mircrobrightfield, Inc., Colchester, VT, USA). Coronal sections were selected to cover the rostral-caudal axis and medial-lateral axes of the isocortex. In each selected coronal section, we measured the cortical surface length. We then selected sites at every 20% distance of the total cortical surface area. That is, we selected evenly spaced sites that are 20%, 40%, 60%, and 80% of the total cortical surface (Fig. 1). If the selected region covered an area of high curvature, we sampled an adjacent region. We then overlaid a grid on the magnified image. The axes of a grid were aligned perpendicular to the isocortical surface and counting boxes (41 µm × 41 µm) were placed at 200–50 µm intervals, between layer I and the cortical white matter. More closely spaced intervals were used for species with small cortical columns (i.e., rodents) relative to species with large cortical columns (i.e., primates) in order to obtain similar samples per unit column across species.

We used the optical disector method (Williams and Rakic 1988; Williams et al. 2003) to estimate neuron numbers contained in each box's volume. The sections were thick enough to employ a 3D, 5 µm thick, guard zone, whereby cells that lay on the 3 exclusion planes (x, y, and z planes) were excluded. We only counted neurons and excluded glial cells. Neurons were distinguished by the presence of coarse and dark stained Nissl substance in the cytoplasm, a distinct nucleus and a pale soma, contrasting with glial cells, which lack a conspicuous nucleolus and endoplasmic reticulum and exhibit a condensed soma (Cahalane et al. 2012).

Measurements of layers were taken orthogonal to the cortical surface area. In our samples, it was difficult to reliably distinguish layers II and III. Moreover, layer IV could not be reliably visualized in some parts of the isocortex (e.g., agranular cortex). In order to systematically compare neuron numbers in various layers across the RC and ML axes of the isocortex, we combined layers II–III and IV in our analyses. Layer V and VI were analyzed together. We therefore only examine how supragranular (layer II–IV), infragranular (layers V–VI) neurons, and their sum vary across the RC and ML axes of the isocortex.

We estimated neuron numbers under a unit of cortical surface area according to the following formula:

$$\text{Estimated neuron number} = \text{total cells counted} \times \frac{1}{\text{asf}} \times \frac{1}{\text{hsf}}$$

where asf = B/D and ssf = H/T

B is the base area of the counting frames, D is the distance between each counting box, H is the height of the optical disector guard zone, and T is the average tissue thickness after histological processing. The

Table 1

Information about specimens used in our analyses, correction values derived from 3D reconstructions of the isocortex, number of sampled sites as well as number of sampled

Species name	Capuchin	Owl monkey	Tamarin	Paca	Agouti	Hamster
Specimen ID	970107A	AT980115A	SM970108B	CP970106A	DA970115	N/A
Sex	F	M	F	M	M	M
Brain weight (g)	62	14	9.09	32.94	14.87	0.93[a]
Hemisphere	Left	Left	Right	Left	Left	Left
Thickness (μm)	60	60	60	60	60	40
Guard zone (μm)	5	5	5	5	5	5
Correction factor range	74.76–98.52%	70.22–99.95%	74–99.94%	58.39–99.25%	80.34–99.46%	97.1–100%
Correction factor mean (SD)	86.4 (7.43)	92.82 (7.73)	93.05 (7.4)	89.43 (9.06)	92 (5.7)	94.5 (6.2)
Number of selected sample sites	16	24	24	28	28	40
Number of selected sections	4	6	6	7	7	8
Total supragranular layer neurons sampled	884	1227	1385	422	473	544
Total infragranular layer neurons sampled	439	424	558	283	387	557

[a]Chalfin et al. (2007).

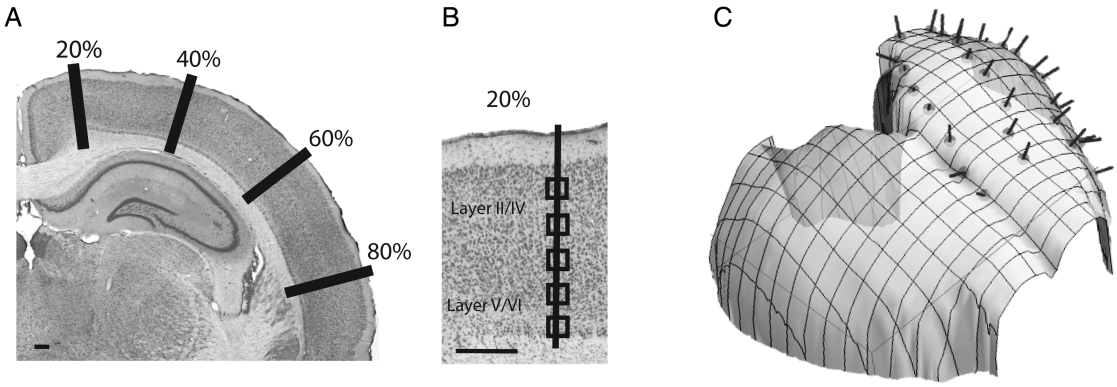

Figure 1. We used the optical fractionator method to estimate neuron numbers in layers II–IV and V–VI in Nissl stained sections under a unit of cortical surface area in 3 rodent and 3 primate species. We systematically sampled sites along the rostro-caudal and medio-lateral axis of the isocortex. (*A*) A coronal section of a hamster Nissl-stained coronal section. The total surface area of the isocortex of the hamster was measured in each serial section and sites were systematically sampled along 20%, 40%, 60%, and 80% of the medio-lateral axis of the isocortical surface. (*B*) Evenly spaced sampled sites were selected orthogonal to the cortical surface area. (*C*) We reconstructed 3D digital models of the isocortex to correct for variations in the curvature of the isocortical surface. The 3D reconstruction of the hamster isocortex is shown here. Scale bar: 1 mm.

estimates of the base area of the counting frames, the distance between each counting box, the height of the optical disector guard zone as well as the average tissue thickness were estimated using the Neurolucida system. We report values for the isocortical neuron numbers for one hemisphere.

To reconstruct total neuron numbers, we used the following formula:

$$\text{Total population} = \text{total cells counted} \times \frac{1}{\text{ssf}} \times \frac{1}{\text{asf}} \times \frac{1}{\text{hsf}}$$

where hsf is the distance between each section.

Correction for Curvature of the Isocortical Surface

The isocortex exhibits curvature along its RC and ML axes, and the presence of gyri and sulci contributes to its curvature. Estimating neuron numbers under a unit of cortical surface area in sections may be compromised if the curvature of the isocortex is not accounted for. That is, the plane of section may not be orthogonal to the cortical surface area and one may thus incorrectly estimate neuron numbers under a unit of cortical surface area. Therefore we calculated the extent to which isocortical curvature influences estimates in our samples. For each isocortex examined, we built a 3D digital model of the cortical surface by assimilating several sources of data (e.g., sagittal or horizontal sections from the alternate hemisphere and views of intact cortical hemispheres from the same species) in order to calculate the curvature correction factor for each location examined.

To digitally reconstruct isocortices, we photographed brain sections as well as the gelatin surrounding the brain. Contours of 15–35 sections of the isocortex and landmarks within the gelatin were made in Adobe Illustrator. Images were binarized, and the surface area was extracted from the sections. From each section, an ordered set of points was selected to characterize the surface of isocortex (typically 50–100 points per section). To represent each cortex's surface, we generated a 3D mesh whose vertices were the selected, ordered points in the aligned sections. The mesh was generated using a combination of Mathematica's TetGenLink functionality for generating 3D tetraedralizations (Mathematica, Version 8.0, Champaign, IL, USA) and an algorithm which utilized the ordering of points within each section to ensure topologically correct reconstructions of the cortical surface. Once the brain was reconstructed in 3D, we located the samples that were used to estimate neuron numbers and used the reconstruction to calculate the normal vector to the cortical surface at each sample's location. We then calculated the curvature correction factor for that site by considering the surface normal vector and the orientation of the coronal plane of section. The curvature correction factor c is given by $c = \cos(\theta)$, where $\theta = \sin^{-1}(n_x/|\vec{n}|)$ is the angle between the surface normal vector $\vec{n}$ and the coronal plane, assumed here to be parallel to the y–z plane of a Cartesian coordinate system. Details of the correction factors for each species examined are listed in Table 1.

Statistical Analysis

We used standard least square regressions to determine whether neuron numbers vary systematically across the RC and ML axes of the isocortex. The significance of the model fit was assessed by comparing the fitted model to a simple mean model with an analysis of variance. We report F values and P values of these tests as well as the adjusted R^2 values of the fitted model. The significance of RC and ML variables as well as the interaction between the 2 variables and the slope derived from the model were compared across species. All statistical analyses were performed in JMP10.

We also use standard least square regressions to compare the scaling of isocortical neuron numbers between the 2 orders. We do not use phylogenetically controlled regressions here because of the relatively small number of species used in the analyses and because reported phylogenetic positions of these species is presently in flux (Murphy et al. 2001; Bininda-Emonds et al. 2007; Blanga-Kanfi et al. 2009), creating uncertainty about the phylogeny that should be used. Given that our nonphylogenetically controlled regression accounts for a large percentage of the variance, it is unlikely that incorporating phylogenetically controlled statistics will change the significance of our results.

Comparing Studies of Neuron and Glial Densities

To determine whether estimates of cortical neuron numbers are influenced by the methods employed, we sought to compare the results of studies addressing neuron numbers in the primary visual cortex (V1) of the macaque. We chose this particular species and cortical area because it has been examined using a variety of methods across multiple studies: O'Kusky and Colonnier (1982) used electron microscopy; Suner and Rakic (1996) used a sample size of 5 rhesus monkeys, performed stereological corrections, and anatomically distinguished neurons from glia; Giannaris and Rosene (2012) used a sample size of 26 rhesus monkeys, performed stereological corrections, and used immunohistochemistry to distinguish neurons from glia. Christensen et al. (2007) used 8 rhesus monkeys to estimate neuron numbers in the occipital cortex (which is principally, but not entirely identical to V1 so the volumes should not be considered identical to V1 volume). Collins et al. (2010, 2013) used sample sizes of 1 and 2 rhesus monkeys respectively, estimated neuron numbers with the isotropic fractionator method and identified V1 in cortical mounts using anatomical landmarks such as gyral patterns. We note that Suner and Rakic (1996) report estimates of total neuron number in macaque V1 but do not report the corresponding measurements of V1 volume in the 5 brains studied. For that reason, we plot the estimated neuron numbers from

Table 2
Total unilateral isocortical neuron numbers estimated in layers II–VI in 3 rodent and 3 primate species

	Capuchin	Owl monkey	Tamarin	Agouti	Paca	Hamster
Layer II–VI neuron numbers	509.63	151.78	112.94	28.85	31.25	4.62
Layer II–IV neuron numbers	363.65	115.86	82.89	16.14	17.45	2.20
Layer V–VI neuron numbers	145.98	35.92	30.05	12.71	13.80	2.42

All values are in 10^6 neurons.

that study against the mean V1 volume (Giannaris and Rosene 2012). We also report the mean and standard deviation of V1 neuron numbers and volumes (Christensen et al. 2007).

We also compare neuron estimates for the cerebral cortex and isocortex obtained with standard stereological techniques with the isotropic fractionator method. Previous reports using the isotropic fractionator method (Gabi et al. 2010; Herculano-Houzel et al. 2011) report neuron numbers for the cerebral cortex and we compare those findings to those obtained with standard stereological techniques.

Results

We estimated isocortical neuron numbers in the granular and supragranular layers (i.e., layers II–IV; designated "supragranular" in the rest of the paper for brevity, although layer IV is always included if present) and infragranular layer neurons (i.e., layer V–VI) in 3 rodent and 3 primate species (Table 2). As overall brain size and isocortex size increases, total isocortical neuron numbers do not increase as fast in rodents as they do in primates (Fig. 2). This is evident from the observation that the slopes of the natural-logged regressions of neuron numbers versus isocortex volume are smaller in rodents ($y = 0.59x + 16.6$; slope confidence interval (CI) ± 0.564; intercept CI ± 0.834) than in primates ($y = 1.24x + 17.608$; slope CI ± 0.007; intercept CI ± 0.009; Fig. 2). The slopes of neuron numbers regressed against cortex volume in rodents fall outside the 95% CIs of primates. Thus, the scaling of neuron numbers versus isocortex size varies between these 2 orders and neuron densities decrease faster in rodents than in primates as overall isocortices enlarge.

We also compare supragranular and infragranular layer neurons scaling in primates and rodents. The linear regressions of supragranular versus infragranular neuron numbers in millions scale with a higher slope within primates ($y = 2.34x + 21.76$; slope CI: ±1.87; intercept CI: ±1.66) than in rodents ($y = 1.35x - 1.05$; slope CI: ±0.16; intercept CI: ±1.74). The resultant slope of the regression equations are greater than 1 within both orders (Fig. 3). Thus, supragranular layer neurons increase disproportionately relative to infragranular layer neurons within both of these orders despite differences in the scaling of neuron densities (Fig. 3).

Variation in Neuron Numbers Across the Isocortex

The lowest neuron numbers per mm^2 of cortical surface area were generally observed in the rostral cortex and the highest were found in the caudal cortex in primates. This trend was observed to a lesser extent in rodents (Fig. 4). To quantify the variation in neuron number across the isocortical sheet within and between species, we examined the ratio of neurons per unit surface area in the most rostral regions to that in the most caudal regions, averaging across the ML axis. We also performed a standard least squares regression of neuron numbers

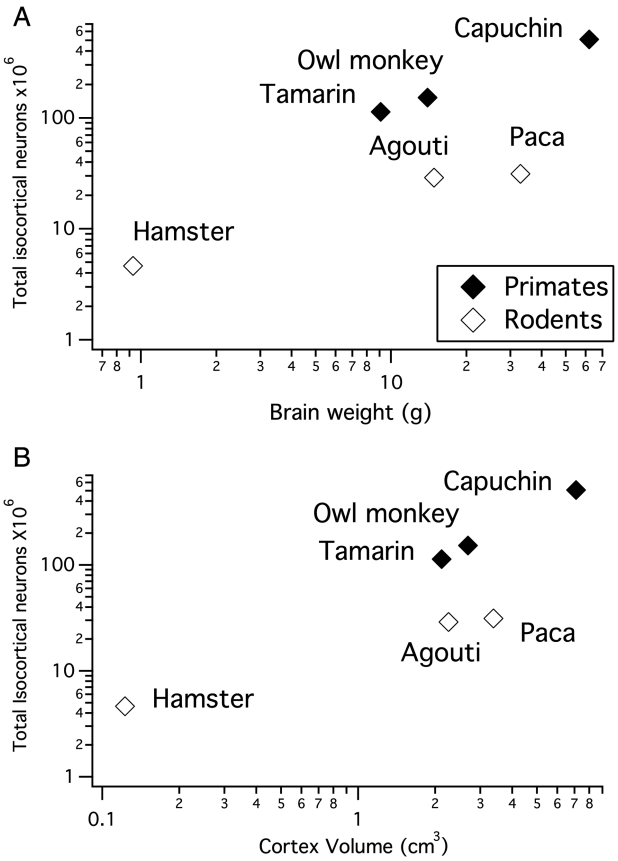

Figure 2. (*A*) Total unilateral isocortical neuron numbers plotted against brain size in primates and in rodents. (*B*) Total unilateral isocortical neuron numbers plotted against cortex volume in primates and in rodents. For a given brain size or isocortex size, rodents exhibit fewer isocortical neurons than primates.

per unit of cortical surface area with the RC and ML axes and an interaction term (RC × ML) as variables to test whether location within the isocortex accounts for a significant percentage of the variance in neuron numbers (Table 3).

In Figures 4 and 5, where species are ordered by total isocortical neuron numbers, we observe that a rostral to caudal gradient in neuron numbers per unit of cortical surface becomes increasingly apparent as total isocortical neuron number increases across species (Table 3). For instance, the capuchin has the most isocortical neurons and their neuron numbers vary by a factor of 2.13, ranging between 56 780 to 120 750 neurons per mm^2 of cortical surface area between the rostral and caudal poles, respectively. The tamarin has fewer isocortical neuron numbers than the capuchin and its neuron numbers vary by a factor of 1.64, ranging between 70 270 and 115 030 neurons per mm^2 of cortical surface area between the rostral and caudal poles (Table 3). The paca has fewer isocortical neurons than the tamarin and its neuron numbers vary by a factor of 1.54, ranging between 25 720 to 39 520 neurons per mm^2 of cortical surface area across the rostral and caudal poles. The hamster has the fewest isocortical neurons of all examined species and its neuron numbers only vary by a factor of 1.15, ranging between 65 550 and 75 100 neurons per mm^2 of cortical surface area across the poles. A difference in neuron density between the rostral and caudal poles is also observed (Table 4; Fig. 6). The standard least square regression accounts for a large percentage of the variance in neuron numbers in

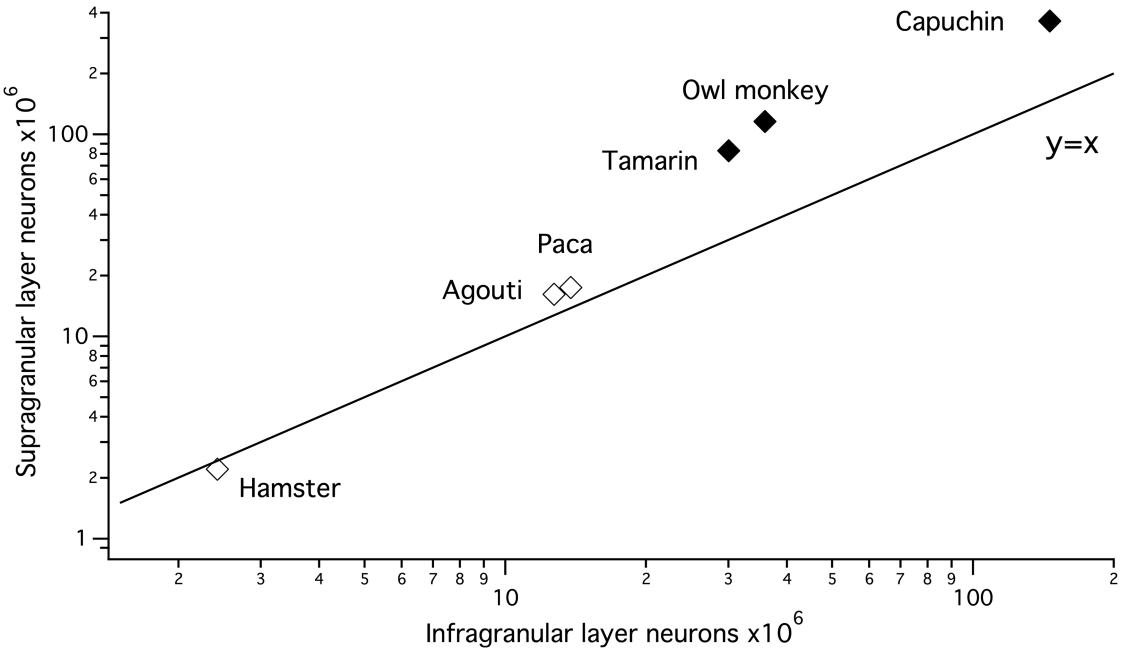

Figure 3. Unilateral supragranular layer neuron numbers increase with a slope >1 in primates and in rodents when regressed against unilateral infragranular layer neurons. Thus, supragranular layer neurons increase faster in numbers than infragranular layer neurons as overall isocortical populations expand across species.

primates (48.34–64.58% of variance) but far less in rodents (2.8–37.9% of variance; Table 3). The percentage of variance is greater in those species with a greater total number of isocortical neurons.

Variation in Supragranular (Layer II–IV) Neurons Across the Isocortex

In most examined species, there is a significant increase in supragranular (i.e., layer II–IV) neurons per unit of surface area across the RC axis (Figs 4 and 6). The ratio of lowest to highest supragranular layer neuron numbers across the isocortical sheet increases from the rostral to caudal poles across species (Fig. 6). For instance, supragranular layer neurons in capuchins exhibit on average 27 820 and 83 920 neurons per mm^2 of cortical surface area and supragranular layer neurons in the hamster range between 23 660 and 44 820 neurons per mm^2 of cortical surface area between the rostral and caudal poles, respectively. The standard least square regression model accounts for between 51.8% and 71.77% of the variance in primates (Table 5) and only between 12.50% and 37.9% in rodents (Table 5). A RC difference in supragranular layer neuron density, across the RC axis is also observed (Fig. 6).

Variation in Infragranular Layer Neurons Across the Isocortex

The variation in infragranular layer (i.e., layer V–VI) neuron numbers is either small or shows a decline from the rostral to caudal pole in both primates and rodents (Figs 4 and 6, Table 4). For instance, infragranular layer neurons increase slightly in the capuchin, ranging between 28 960 and 36 830 neurons per mm^2 of cortical surface area between the rostral and caudal poles whereas infragranular layer neurons decrease in the hamster, ranging between 41 880 and 30 280 neurons per mm^2 of cortical surface area between the rostral and caudal poles (Table 4). The standard least square regression model accounts for only a small percentage of the variance in both orders (22.48–35.13% in rodents and 14.5–22.48% in primates, Table 6). Neuron densities too vary relatively little between the rostral and caudal poles, which is in contrast to the large variation observed in supragranular layer neuron density. Thus, supragranular layer neuron numbers rather than infragranular layer neurons account for most of the cross-cortex variation in the total number of neurons per mm^2 of surface area.

Comparison of Cortical Volumes, Neuron Numbers, and Glia Numbers Across Studies Using Different Techniques

The primary visual cortex (V1) in the macaque is the single cortical area that has been the focus of a large number of quantitative studies aimed at establishing neuron numbers (Fig. 7). The 3 studies using sectioned material with stereological correction (Suner and Rakic 1996; Christensen et al. 2007; Giannaris and Rosene 2012) yield consistent cortical volume, neuron numbers (Fig. 7), neuron density, and neuron/glia ratios. Of the remaining studies, the estimate of total neuron number derived by O'Kusky and Colonnier (1982) can be discounted for the lack of stereological correction, though their reported ratio of neurons to total cells (66%) is similar to other reports. The 2 estimates of total neuron numbers produced by the isotropic fractionator method (Collins et al. 2010, 2013) are notable outliers, reporting ~50% of the total neuron numbers reported by the other investigators. The neuron/total cell ratio reported by Giannaris and Rosene (2012) is 66%, Christensen et al. (2007) 62%, and Collins et al. (2010, 2013) 40%. Both neural and glia counts reported by the isotropic method are reduced but the neuron numbers exhibit the largest difference between methods.

Comparing estimates of total unilateral isocortical neurons in the macaque produces a similar contrast. Using stereology, Christensen et al. (2007) estimated neuron numbers in the rhesus monkey's isocortex to be 1350 million. Lidow and Song

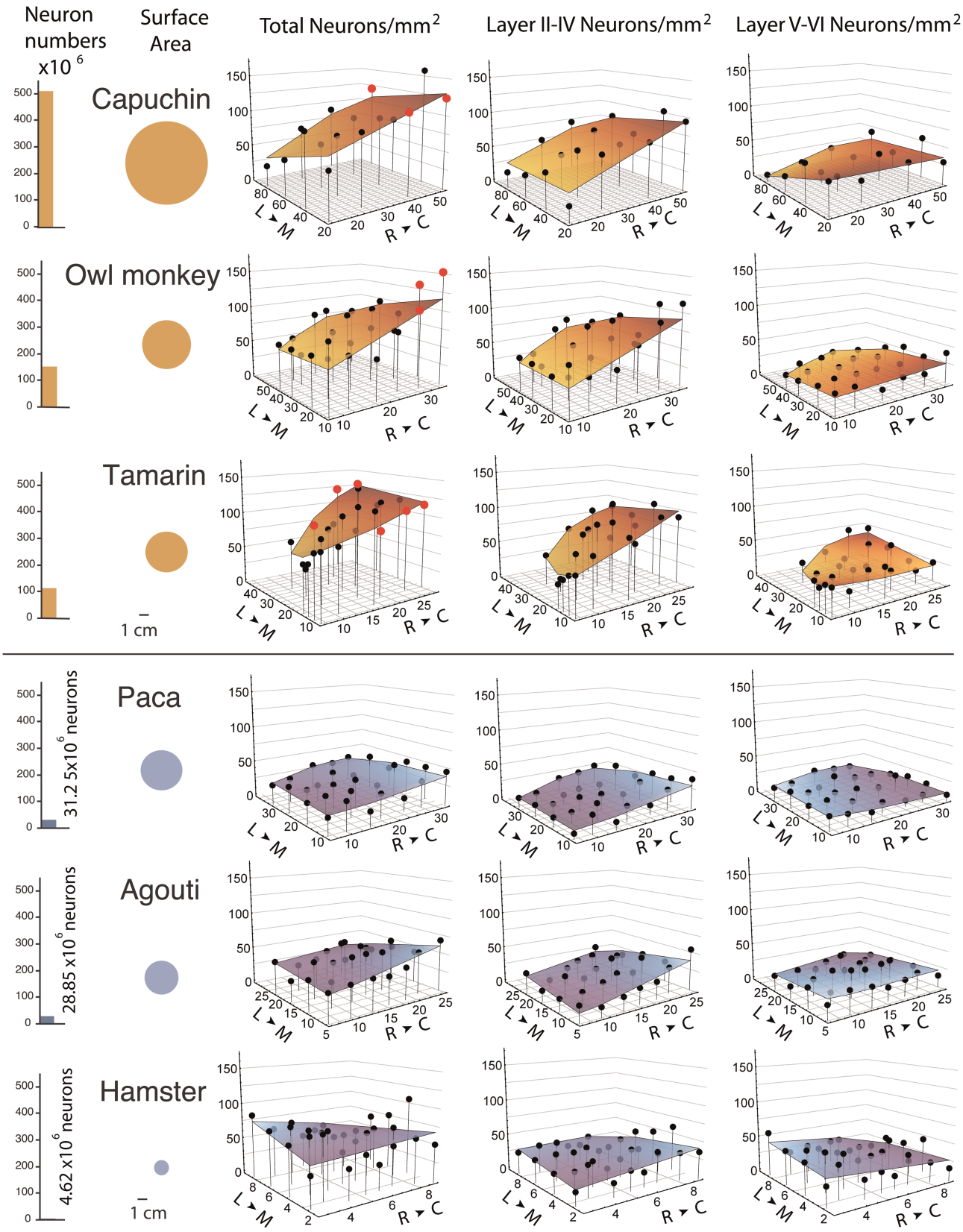

Figure 4. Total isocortical neurons and isocortical surface area are shown on the left. Total neuron numbers as well as supragranular (layer II–IV) and infragranular (layer V–VI) neuron numbers per mm^2 of cortical surface in the capuchin, owl monkey, tamarin, paca, agouti, and hamster are plotted against the (RC) rostro-caudal axis and (ML) medio-lateral axes of the isocortical sheet. The rostro-caudal and medio-lateral axes are displayed in millimeters. Data points from primary visual cortex (V1) of primates are shown in red.

Table 3

Parameter estimates for a standard least square regression of neuron numbers per mm^2 of cortical surface area with the rostro-caudal (RC) and medio-lateral (ML) axes as well as the interaction between these 2 variables (RC × ML) as variables

	Variance		Intercept		RC		ML		RC × ML	
Species	%	*F*	Value (SE)	*t*	Slope (SE)	*t*	Slope (SE)	*t*	Slope (SE)	*t*
Capuchin	62.95	9.49**	63 597.18 (15 723.04)	4.04**	1.56 (0.32)	4.84***	−0.54 (0.23)	−2.38*	6.3568e^6	0.42
Owl monkey	48.34	8.17**	51 856.27 (11 790.43)	4.40***	1.89 (0.42)	4.52***	−0.44 (0.27)	−1.61	−2.67e^{-5}	0.41
Tamarin	64.58	14.98**	4 6099.63 (8667.30)	5.32***	3.34 (0.51)	6.59***	−0.85 (0.32)	−2.63*	0.0001	2.59*
Paca	12.86	6.49**	22 517.73 (4760.14)	4.73***	0.42 (0.18)	2.33*	−0.001 (0.17)	−0.01	−1.968e^{-5}	−0.92
Agouti	37.90	2.32	39 694.19 (4846.58)	8.19***	0.65 (0.25)	2.63*	−0.52 (0.24)	−2.14*	−0.0001	−2.67*
Hamster	2.80	1.29	64 744.03 (11 703.54)	5.53***	−1.33 (1.60)	−0.83	0.51	1.32	−0.001	0.001

Only SEs >0.0001 are reported.

SE, standard error.

*$P < 0.05$, **$P < 0.01$, ***$P < 0.001$.

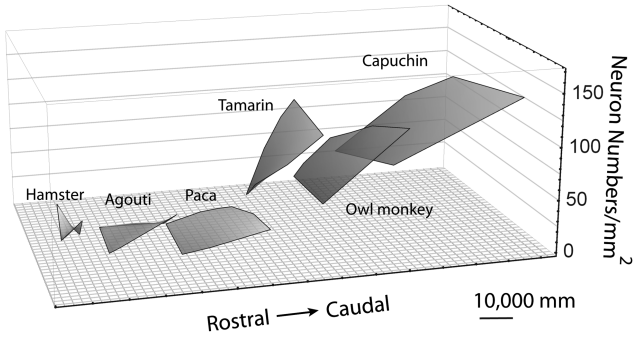

Figure 5. Total neuron numbers per mm^2 of cortical surface area in primate and rodent species are shown on a single graph. Primates exhibit a steeper slope in neuron numbers per mm^2 of cortical surface area when regressed against the (RC) rostro-caudal and (ML) medio-lateral axes of the isocortical sheet compared with rodents. The RC and ML axes are in millimeters. The plotted surfaces are shifted on the rostro-caudal axis for better visibility.

(2001) estimate 2950 million neurons in the rhesus monkey isocotex. In contrast, studies using the isotropic fractionator method (Gabi et al. 2010; Herculano-Houzel et al. 2011) report ~825 million neurons for the unilateral cerebral cortex of the rhesus monkey.

For another contrast, the pattern of scaling of neuron numbers for rodents versus primates can be compared between studies using the isotropic fractionator and the present study (Gabi et al. 2010; Herculano-Houzel et al. 2011). For the isotropic fractionator, estimated neuron numbers in the "cerebral cortex" between primates and rodents. The "cerebral cortex" includes the hippocampus, entorhinal and olfactory cortices, and various basal forebrain nuclei (Fig. 8). Thus, Figure 8 unavoidably contrasts both the set of forebrain structures included, and the method of analysis of neuron numbers. Given the inclusion of large structures such as the hippocampus and olfactory cortices, it would be expected the neuron numbers reported with the use of the isotropic fractionator method (Gabi et al. 2010; Herculano-Houzel et al. 2011) studies should be higher than those reported in the present study which reports only on isocortex. The difference should be particularly large for rodents, as these structures comprise a much greater percentage volume of the forebrain in rodents, progressively greater in larger rodent brains (Inset, Fig. 8). This prediction is what is seen in Figure 8: the values reported for primates are somewhat lower, and the values for rodents are much lower when only isocortex is included. The general concordance of total neuron number estimates in the primarily New World primates between both studies suggests that the macaque VI estimate is erroneous or anomalous in some fashion.

Discussion

Our main finding is of a rostral to caudal increase in neuron numbers per cortical column, which is most pronounced in primates but varies with total isocortical neuron numbers in both rodents and primates. Most of this variation in neuron numbers is produced by changes in supragranular layer neuron numbers across the isocortical sheet. The neuron numbers per unit of cortical surface area are the result of species, RC cortical location and their interaction, and can approach a 3-fold difference across the cortex and between species. We compare our findings to previously published studies and consider the implications of our results in the context of known developmental timing gradients.

Inspection of total neuron numbers under a unit of cortical surface area (Figs 4 and 5) shows that smaller cortices are more uniform in neuron numbers across the isocortex, but larger ones show an increasingly pronounced elevation in the caudal pole. It is well known that the primary visual cortex has more neurons than other cortical regions in primates (Rockel et al. 1980; Dehay et al. 1993; Kennedy and Dehay 1993; Collins et al. 2010, 2013), and we considered the possibility that the trends we report are principally due to the difference in primary visual cortical neurons relative to the rest of the isocortex. However, only a small fraction of the samples come from the primary visual cortex for primates, and if V1 is excluded from consideration, the gradient persists (Fig. 4). Thus, the variation in neuron numbers is not only due to differences in the primary visual cortex versus the remaining brain regions.

Methodological Issues in Counting Cortical Numbers

The persisting discrepancies in the claims about the uniformity, or lack thereof, in the number of neurons per cortical column thus have multiple sources. We have attempted to ascertain the methodological versus empirical causes of these different claims. We first discuss the basic issue of enumerating cells. The use of "assumption-based" or "model-based" stereology was commonly used approximately 50 years ago (Abercrombie 1946), which is reasonably accurate for the section thicknesses and cell sizes employed for light microscopy (Benes and Lange 2001). Several versions of more contemporary stereology,

Table 4
Mean and standard errors of neuron numbers in the most rostrally and most caudally selected regions of the isocortex in the 6 species

Species	Region	Total neuron number mean (SE)	Supragranular neuron number mean (SE)	Infragranular neuron number mean (SE)
Capuchin	Rostral	56 783.5 (28 894.65)	27 820.43 (6294.70)	28 963.07 (9844.5)
	Caudal	120 755.5 (32 403.6)	83 925.26 (9719.88)	36 830.25 (7613.7)
	Varies by	2.13	3.02	1.23
Owl monkey	Rostral	67 372.5 (6922.97)	47 130.78 (5282.93)	20 241.74 (2498.70)
	Caudal	116 073.98 (16 084.3)	87 345.82 (27 771.39)	28 728.16 (4452.84)
	Varies by	1.72	1.85	1.42
Tamarin	Rostral	70 272.84 (5812.74)	39 745.59 (4722.17)	30 527.26 (1824.03)
	Caudal	115 029.31 (5978.19)	88 673.79 (5105.99)	26 355.52 (6778.49)
	Varies by	1.64	2.23	0.86
Paca	Rostral	25 721.38 (2891.5)	9518.16 (1929.46)	16 203.22 (1501.33)
	Caudal	39 521.35 (47 494)	29 852.47 (4540.25)	96 68.87 (1738.39)
	Varies by	1.54	3.09	1.67
Agouti	Rostral	34 647.33 (3398.15)	17 117.92 (2813.66)	17 529.4 (2390)
	Caudal	43 291.2 (9214.58)	30 674.36 (18 574.34)	12 616.83 (2370.53)
	Varies by	1.25	1.79	0.72
Hamster	Rostral	65 546.65 (19 992.13)	23 661.89 (3204.45)	41 885.06 (7102.18)
	Caudal	75 101.37 (23 312.91)	44 824.39 (5819.94)	30 277.13 (12 272.09)
	Varies by	1.15	1.89	0.72

wherein no assumptions about symmetry or shape of counted entities are made are represented in the sources cited here (Suner and Rakic 1996; Giannaris and Rosene 2012). The introduction of the isotropic fractionator and flow-cytometry techniques allow the assessment of cell numbers in large volumes of tissue. However, the comparability of neuron counts as reconstructed from sectioned material with those obtained from the isotropic fractionator technique has not been examined previously.

In the studies of macaque striate cortex we reviewed, the work of Giannaris and Rosene (2012) must represent the gold standard, due to its large sample size ($n = 26$), identification of striate cortex boundaries in sectioned material, stereological correction of counts, optimal volume reconstruction techniques, and the use of immunohistochemical identification of neurons versus glia. Nevertheless, the studies missing 1 or 2 of these features (Suner and Rakic 1996; Christensen et al. 2007) do not fare badly, producing very similar neuron numbers with respect to cortex volume (Fig. 7) and near-identical neuron/glia ratios. The isotropic fractionator assessment of the macaque striate cortex is divergent from all the other studies, producing on the one hand the largest striate volumes in the 40 individual animals considered, and on the other the lowest neuron numbers. A possible cause of error in neuron counts made via the isotropic fractionator is that occasional accidental defects in nuclear membrane integrity or immunohistochemical labeling can produce an undetected but anomalously low counts. This would suggest that a sample of sectioned material should be processed in parallel with the isotropic fractionator technique to verify labeling and tissue quality. Across the cortical sheet for any particular species, the relative numbers of neurons per unit of surface area appear to be reasonably consistent across the 2 techniques (Collins et al. 2010; Cahalane et al. 2012; this study).

A second issue is reconciliation of the claims of uniformity in neuron numbers per cortical column as originally reported by Rockel et al. (1980) and more recently by Carlo and Stevens (2013) using stereological techniques, in mouse, rat, cat, and monkey (omitting visual cortex which is known to have more neurons per column). Examination of the surface plots of neuron number per unit of cortical surface area in Figure 4 produces a clear answer—the cortical areas chosen for assessment in these 2 studies (Rockel et al. 1980; Carlo and Stevens 2013) were deliberately located in the middle of the cortical surface, both to study primary sensory areas, and to avoid areas of high curvature at the rostral and caudal regions. The mean values of about 100 000 neurons under an area of 1 mm^2 conform well to the values we measured in the middle of the cortical surface (Fig. 4). Choosing sites that lie in the middle of the rostral to caudal gradient eliminates exactly those areas where neuron numbers diverge most from mean values. In addition, the choice of species in prior studies was not intended to explore the range of species variation within taxa, as it is in the present study.

Overall Scaling of the Cortex in Rodents Versus Primates

Many different features of brain organization have been compared in studies of brain allometry: the volume of whole brains, to detailed volumes of identified structures, to counts of neurons, neuron types, and glia. A full understanding of brain scaling requires the integration of information gleaned at all these levels.

Considering cortical volume alone, the cortex has long been known to scale with positive allometry relative to core brain parts, coming to occupy the majority of volume in the largest brains. Anthropoid primates have a "grade shift" in cortical volume. That is, the isocortex is a larger proportion of brain volume at every brain size relative to insectivores (Stephan et al. 1981). While early studies hypothesized that the grade shift in cortex volume was a feature specific to primates, more extensive studies of the mammalian phylogeny have shown that variation in this feature is widespread, both between and within taxonomic groups (Reep et al. 2007; Workman et al. 2013). Moreover, the isocortex, hippocampus, and limbic structure volumes each scale with different slopes relative to overall brain size, and considering primates compared with other taxonomic groups each structure's slopes are further modified (Finlay and Darlington 1995; Reep et al. 2007).

Considering organization at the cellular level, the scaling of the neuron cell body, neuropil, and glial components within each brain structure yields an additional source of variation in how structure volumes scale with increasing neuron numbers. The cytoarchitecture of a structure, for example, whether the cellular organization is nuclear or laminar and whether neurons are close-packed or embedded in extended neuropil,

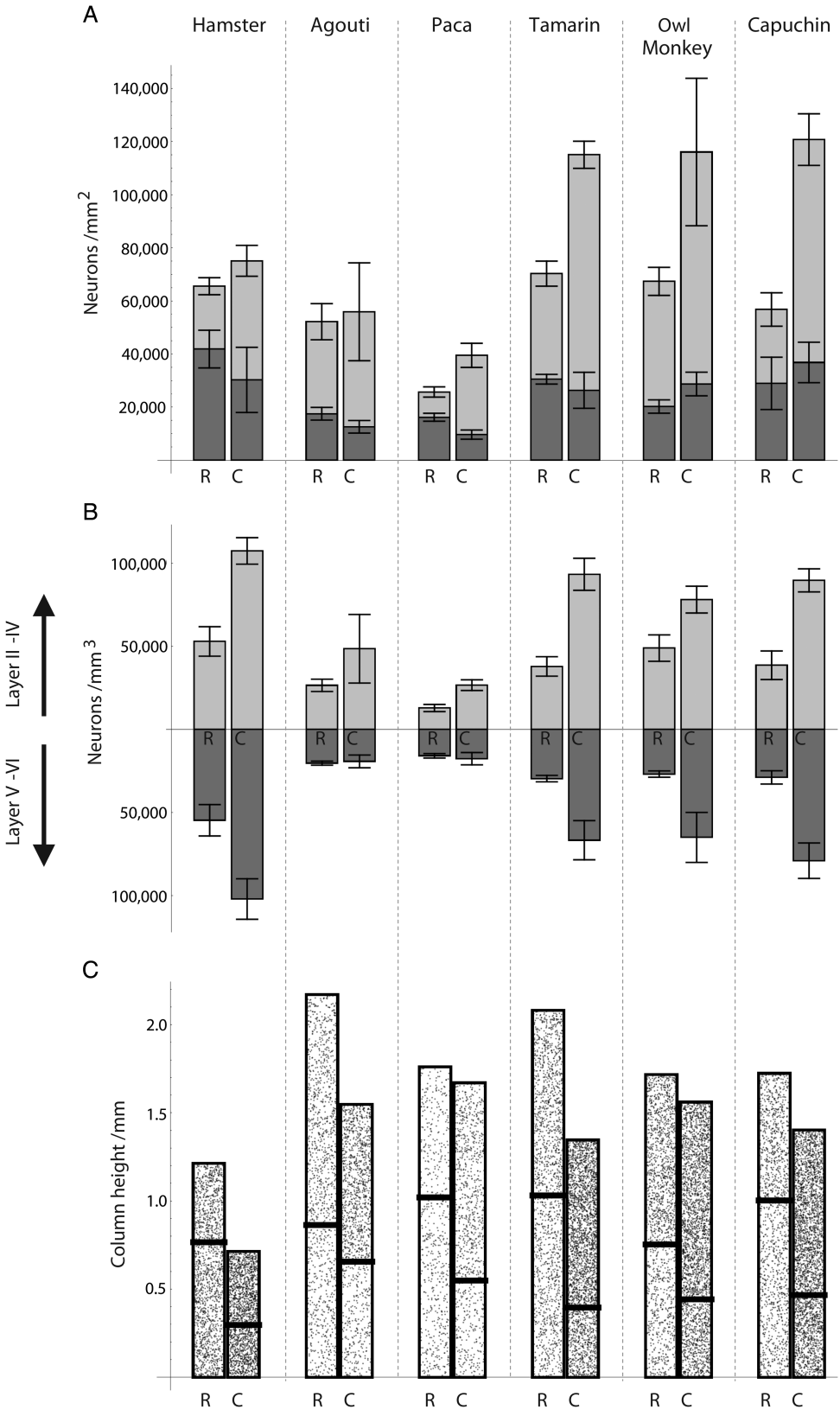

Figure 6. (*A*) Neuron numbers (in supragranular and infragranular layers) per mm^2 of cortical surface area in the rostral and caudal poles of the isocortex. Species are ordered by total number of isocortical neurons. Species with more isocortical neurons exhibit a greater range of variation in neuron numbers under 1 mm^2 of cortical surface between the rostral and caudal poles. The range of variation in infragranular layer neurons is relatively small in primates and in rodents. The error bars indicate the standard errors for the respective layers (not for the total number of neurons in the column) (*B*) Density of neurons at the rostral and caudal poles in supra- (plotted on top) and infragranular layers (plotted at bottom). The range of variation in neuron numbers is similar to the range of variation in neuron density between the rostral and caudal poles across species. (*C*) A visualization of the implied height of the cortical columns, within the layers of which the stipple density is proportional to neuronal density, shows a rostro-caudal decrease in column height.

Table 5
Parameter estimates for a standard least square regression of supragranular layer neuron numbers per mm^2 of cortical surface area with the rostro-caudal (RC) and medio-lateral (ML) axes as well as the interaction between these 2 variables (RC × ML)

	Variance		Intercept		RC		ML		RC × ML	
Species	%	*F*	Value (SE)	*t*	Slope (SE)	*t*	Slope (SE)	*t*	Slope (SE)	*t*
Capuchin	69.4	12.34**	26 895.25 (10 637.84)	2.53*	1.28 (0.21)	5.85***	−0.17 (0.15)	−1.10	$-7.28e^{-6}$	−0.73
Owl monkey	51.8	9.25**	29 851.36 (10 001.74)	2.98***	1.76 (0.36)	4.94***	−0.23 (0.23)	−1.03	−0.00002	−0.84
Tamarin	71.77	16.95**	26 213.69 (7521.74)	3.49***	3.04 (0.44)	6.91***	−0.73 (0.28)	−2.58**	3.57e−5	0.93
Paca	12.86	2.32	6578.73 (3822.36)	1.72	0.69 (0.14)	4.72***	−0.09 (0.14)	−0.63	$-1.75e^{-5}$	−1.02
Agouti	37.9	6.49**	12 455.9 (3817.48)	3.26**`	0.83 (0.19)	4.27**	−0.13 (0.19)	−0.70	$-9.13e^{-5}$	−2.99**
Hamster	12.50	2.47**	20 391.12 (6559.80)	3.11**	1.44 (0.89)	1.62	0.04 (0.74)	0.05	−0.0008 (0.0004)	−2.03

Only SEs >0.0001 are reported.
SE, standard error.
*$P < 0.05$, **$P < 0.01$, ***$P < 0.001$.

Table 6
Parameter estimates for a standard least square regression of infragranular layer neuron numbers per mm^2 of cortical surface area with the rostro-caudal (RC) and medio-lateral (ML) axes as well as the interaction between these 2 variables (RC × ML)

	Variance		Intercept		RC		ML		RC × ML	
Species	%	*F*	Value (SE)	*t*	Slope (SE)	*t*	Slope (SE)	*t*	Slope (SE)	*t*
Capuchin	35.13	3.70*	36 701.93 (9258.36)	3.96***	0.28 (0.19)	1.49	−0.37 (0.13)	−2.78*	$1.38e^{-5}$	1.56
Owl monkey	33.38	3.14*	220 004.91 (4140.64)	5.31***	0.14 (0.15)	0.37	−0.20 (0.09)	−2.11*	$-3.62e^{-6}$	−0.32
Tamarin	22.48	1.77	18 885.94 (4891.09)	4.07***	0.30 (0.28)	1.06	−0.13 (0.18)	−0.69	$7.8e^{-5}$	3.14
Paca	22.48	3.60*	15 939 (2185.61)	7.29***	−0.26 (0.08)	−3.17**	0.08 (0.08)	1.08	$-2.21e^{-6}$	−0.23
Agouti	14.5	2.53*	27 238.28 (3530.78)	7.71***	−0.19 (0.18)	−1.01	−0.28 (0.18)	−2.18*	−0.000012	−0.43
Hamster	19.90	3.57*	44 352.84 (6696.75)	6.62***	−2.77 (0.91)	−3.04**	0.47 (0.76)	0.63	−0.0005 (0.0004)	−1.18

Only SEs >0.0001 are reported.
SE, standard error.
*$P < 0.05$, **$P < 0.01$, ***$P < 0.001$.

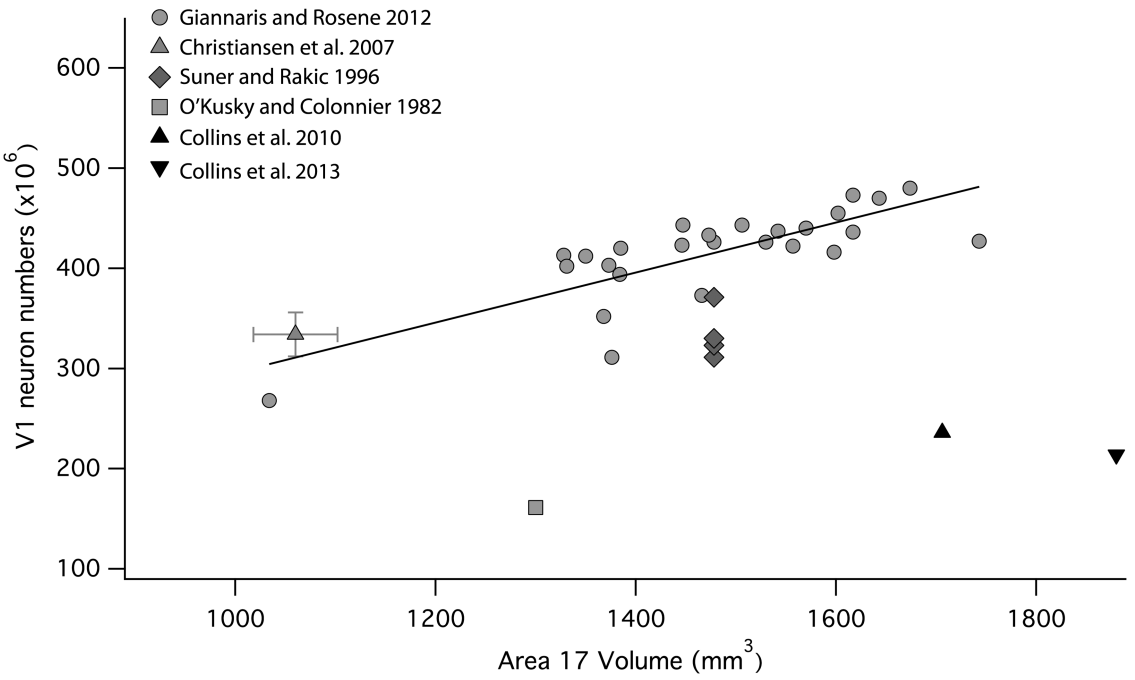

Figure 7. Estimates of V1 neuron numbers assessed with the use of the optical disector and the istroptic fractionator methods plotted against V1 volume. The estimates obtained from the optical disector method are much higher than that estimated with the isotropic fractionator method. Data from Christensen et al. (2007) show 1 standard deviation for the estimated V1 volume and estimated V1 neuron numbers. Shown here are values for one hemisphere.

has direct consequences for its volume scaling. Different connectional architectures have very different implications for how much volume must be devoted to axons and dendrites in order to maintain connectivity as neuron number increases. The volumetric consequences of inefficient scaling of connectivity can be so extreme (Murre and Sturdy 1995; Klyachko and

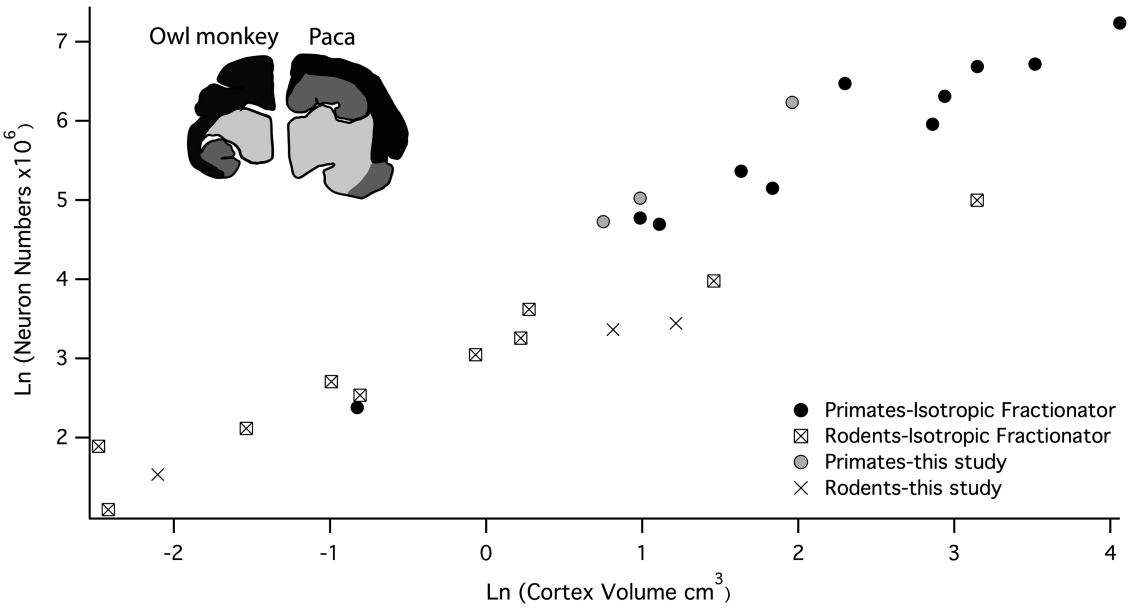

Figure 8. Unilateral cerebral cortical neuron numbers estimated with the use of the isotropic fractionator method are plotted against cerebral cortex volume and isocortical neuron numbers from the present analysis are plotted against isocortical volume. Estimates obtained with the isotropic fractionator method includes the isocortex (depicted in black in the agouti and paca) a number of limbic structures (depicted in dark grey), which are known to differ in size between these 2 taxonomic groups (Reep et al. 2007; this study). Data on primates are from Herculano-Houzel et al. (2007) and Gabi et al. (2010). Data on rodents are from Herculano-Houzel et al. (2011). Cerebral cortex volume was estimated by dividing the weight by 1.036 to reconstruct volume.

Stevens 2003) that there must be strong selection on the developmental control of the topography of axon outgrowth. The topography of connections holds implications not only for the volumetric scaling of a structure but also for information processing at multiple levels. In particular, studies have found evidence that the topography of axon outgrowth in the cortex may have evolved to exploit the "small world" principle of network connectivity (Watts and Strogatz 1998; Kaiser and Hilgetag 2006; Modha and Singh 2010; Cahalane et al. 2011). A "small world" brain network is one in which the distribution of the lengths of axons calls for mostly short axons, while a small complement of lengthy axons under the distribution's long "tail" ensures that only a short chain of axons is required to connect any 2 neurons. Apart from maintaining efficient network connectivity (i.e., short paths between neurons), being comprised of mostly short axons makes such a pattern volume efficient too.

As to the scaling of the relative and absolute numbers of neurons and glia versus structure size, previous studies using the isotropic fractionator method have found that rodents have different "cellular scaling rules" than primates (Gabi et al. 2010; Herculano-Houzel et al. 2011). From the data presented in these studies, however, it is not clear whether the different "scaling rules" result from the aggregate of regions included in the analysis or from a scaling principle that spans the entire aggregate. These brain regions each exhibit different allometries in rodents versus primates by structure and also have vastly different cellular architectures, so the value of analyzing them in aggregate is not obvious.

In the present study, considering the isocortex alone, however, it is clear that neuronal density decreases in large rodent isocortices while primate neuronal density remains relatively constant, independent of brain size. To illustrate the differences in scaling across the 2 orders, we calculated the volumes predicted for the primate's isocortices if isocortical neuronal density versus number of isocortical neurons were to scale in primates according to the same rule as is implied by our 3 rodent data points (extrapolated linearly): the tamarin and capuchin, respectively, would have isocortices 17 times and 100 times larger than their empirical volumes. There are several potential sources of this difference that are not necessarily independent. First, the neurons in primates could simply be smaller, consistent with the whole body "miniaturization" that is a feature of New World primates (Hanken and Wake 1993). A second possibility is that the ratio of neuropil to neuronal cell bodies could be lower. Such a difference between rodent and primate orders could be due to different volume requirements arising from altered patterns of neuronal connectivity. For example, there may be a change in the distribution of axon lengths from a normal or exponentially decaying distribution to a longer-tailed distribution (but having a relatively lower mean), whereby the primate order avails of "small-world" connectivity to a greater extent (Cahalane et al. 2011). The result would be a reduced scaling exponent for the volume requirement of connectivity as neuron numbers increase in primates. Finally, the ratio of glia to neurons could be lower in primates. Distinguishing between the first 2 possibilities is not a simple matter, and the number of glia has been linked to neuron size and axon length (Friede 1963). In summary, it is currently not clear that the neuron numbers in the isocortex scale in any intrinsically different way between primates and rodents, but merely that rodent neurons are larger or associated with more neuropil as their isocortical neurons expand.

Local, Global, and Species-Level Differences in the Cortical Sheet

We systematically sampled sites across the entire isocortical sheet, without the identification of areas, in order to better relate to the developmental literature. In making this choice,

we do not discount the importance of cortical areas. Rather, we focus on features best described by paying attention to the cortical surface as a whole and that approach, in turn, may better highlight traits which are unique to particular areas. For example, a previous analysis found that primary cortical areas have increased neuron numbers per unit surface area relative to association areas even after accounting for the rostral to caudal gradient in neuron numbers (Cahalane et al. 2012). On the evidence of prior developmental studies, we identified reduced early cell death in those regions as being a possible mechanism imprinting this area-specific trait upon the more general landscape established by the rostral-caudal gradient (Finlay and Slattery 1983).

Regarding species level differences, putting aside the fact that neuronal density varies between rodent and primate isocortices, it is interesting that when neuron numbers alone are considered, the supragranular population grows with positive allometry with respect to the infragranular layers in both orders. In those species where a rostral to caudal increase in neuron number exists, it is due to an increase in the neuron population in supragranular rather than the infragranular layers (Fig. 4). We cannot rule out the possibility that there is a small grade shift in supragranular neuron numbers relative to infragranular neuron numbers between rodents and primates because of our small sample size (Fig. 3). It is therefore not clear whether the common ancestor of primates and rodents had differences in neuron numbers in supragranular or infragranular layers per unit of cortical surface area (Rakic 2009). However, the similarity of the 2 patterns at their different scales hints that underlying the trends may be a developmental mechanism that is conserved across species.

Developmental Mechanisms Accounting for Overall Isocortical Scaling

We hypothesize that a known rostral-to-caudal gradient in neurogenesis timing (Smart 1983; Bayer and Altman 1990, 1991; Lent et al. 1990; Miyama et al. 1997; Rakic 2002; Suter et al. 2007; Caviness et al. 2009) during development is the source of the systematic variation in neuron numbers across the isocortex, which we have described in this study. In addition, an infragranular-to-supragranular layer gradient has also been documented, whereby the superficial layers of the isocortex are populated by neurons, which are typically generated after those populating the deeper layers. In what follows we briefly review the details and import of both these developmental gradients. We posit that their combined action is the source of both the rostral to caudal change total neuron numbers and the accompanying shift in the ratios of upper layer to lower layer neurons.

Although little is known about developmental cell cycle kinetics in the species we selected in this study (e.g., paca, agouti, tamarin), there is ample evidence to suggest that the relative duration of neurogenesis and gradients in neurogenetic schedules can account for patterns in phylogenetic variation in brain size and neuron numbers. This is known to be the case in mammals and in birds (Finlay and Darlington 1995; Finlay et al. 1998; Clancy et al. 2001; Chenn and Walsh 2002; Striedter 2005; Charvet and Striedter 2008, 2011; Striedter and Charvet 2008; Dyer et al. 2009; Charvet et al. 2011; McGowan et al. 2012; Workman et al. 2013). Therefore, although specific data about the length of developmental schedules for most of the species examined here is largely lacking, there is no reason to assume the species described here should depart from the general mammalian pattern established in other primates and rodents.

The presence of a gradient in the duration of neurogenesis, from the rostral to caudal poles of the developing isocortex, has been well established in both primates and rodents (Smart 1983; Bayer and Altman, 1990, 1991; Miyama et al. 1997; Rakic 2002; Suter et al. 2007; Caviness et al. 2009). In the rhesus monkey, for instance, terminal neurogenesis generally occurs earlier in the rostral isocortex and last in the caudal isocortex (Rakic 1974, 2002). Cortical neurogenesis begins at approximately embryonic day 38–40 throughout the isocortex in rhesus monkey (Rakic 2002). Neurogenesis in the rostral cortex (e.g., motor cortex) ends slightly before embryonic day 80, whereas, more caudally, neurogenesis ends slightly before embryonic day 100 in the somatosensory cortex and on embryonic day 102 in area V1 at the most caudal pole (Rakic 1974, 2002). There is some departure from the overall, rostral to caudal trend in neurogenesis timing: for example, a rostral region of the isocortex, A46, ends neurogenesis after the motor cortex even though A46 lies rostral to the motor cortex (Rakic 2002). Although it is much reduced in overall duration, a similar schedule, whereby neurogenesis proceeds for longer in caudal regions, has been described both for mouse (Miyama et al. 1997; Suter et al. 2007; Caviness et al. 2009) and rat (Bayer and Altman 1990, 1991). The expected import of this gradient is that total neuron numbers would be higher in caudal regions.

In development, supragranular layer neurons are born after infragranular layer neurons (Rakic 1974, 2009; Clancy et al. 2001). As neurogenetic schedules lengthen, the pool of progenitor cells that will give rise to supragranular layer neurons should expand relative to the progenitor pool that will give rise to infragranular layer neurons (Finlay and Darlington 1995; Charvet et al. 2011). Accordingly, extension of developmental schedules should result in a disproportionate expansion of supragranular versus infragranular layer neuron numbers. We have found that supragranular and infragranular layer neurons scale similarly in both rodents and primates, and that the number of supragranular layer neurons scales with a slope >1 when regressed against the number of infragranular layer neurons. These finding are consistent with the view that developmental schedules across species give rise to disproportionate but predictable changes in the compliments of neurons assigned respectively to the upper and lower layers of the isocortex.

We hypothesize that it is the combined actions of the infragranular-to-supragranular and the rostral-to-caudal gradients of neurogenesis that cause supragranular layer neurons rather than infragranular layer neurons to contribute to the variation in total neuron numbers per mm^2 of cortical surface area. As developmental schedules lengthen, supragranular layer neurons that are born late in development should become disproportionately more numerous relative to infragranular layer neurons, which are produced earlier (Finlay and Darlington 1995; Charvet et al. 2011). Given that neurogenesis proceeds for longer at the caudal pole, it would be expected that supragranular layer neurons become disproportionately more numerous at the caudal pole relative to their compliment at the rostral pole—and this is exactly what we have observed empirically.

Finally, we consider how changes to the duration of cortical neurogenesis across species account both for changes in the difference in the proportion of supra- to infragranular layer neurons and for the fact that the gradient in neuron numbers is more pronounced in larger isocortices. Neurogenesis ends later in caudal regions even in small isocortices; however, the difference in timing between terminal neurogenesis in rostral versus caudal cortex is known to be reduced in smaller cortices, whether expressed in units of absolute time or as a fraction of the developmental interval. For example, the timing of terminal neurogenesis across different areas varies by as much as 3 weeks in the rhesus monkey (Rakic 2002) whereas such a variation along the RC axis is much harder to discern in small rodents, being a matter of a day or 2 at most (Bayer and Altman 1990, 1991; Miyama et al. 1997). Therefore, prolonging isocortical developmental schedules appears to increase the difference between the timing of neuronal birth in the rostral versus the caudal cortex. For that reason, we expect greater variation in total number of neurons from the rostral to caudal poles of isocortices with longer developmental intervals. Moreover, this model implies that a larger isocortex would have a greater fraction of supragranular versus infragranular neurons. That is, relatively more numerous "late-born" neurons are more likely destined for the superficial layers. The specifics of these species differences in cell cycle kinetics have yet to be investigated empirically.

Summary

We found systematic variation in neuron numbers along the rostral-caudal axis of the isocortex, the variation becoming more pronounced in species with large cortices. We find that most of the variation in neuron numbers per mm^2 of cortical surface area is accounted for by variation in supragranular layer neuron numbers. These patterns can be related to well-established developmental gradients in neurogenesis in the isocortex. Varying gradients in cell cycle kinetics may be a common mechanism producing diversity in the cellular make-up of brain tissue not only across species but also across the brain.

Funding

This work was supported by National Science Foundation/Conselho Nacional de Desenvolvimento Cientifico e Tecnologico (grant 910149/96-99) to Luis Carlos de Lima Silveira and a National Science Foundation (grant IBN-0138113 to B.L.F.). This work was also supported by an NIH fellowship (F32HD0 67011 to C.J.C.), a National University of Ireland Traveling Studentship to D.J.C., as well as a National Science Foundation (grant CCF-0835706) to Steven Strogatz. The content is solely the responsibility of the authors and does not necessarily represent the official views of any supporting agency.

Notes

We thank Luiz Carlos de Lima Silveira for sponsorship of the New World Monkey study in which the sectioned material was collected and Peter Kaskan for brain histology. *Conflict of Interest*: None declared.

References

Abercrombie M. 1946. Estimation of nuclear populations from microtome sections. Anat Rec. 94:239–247.

Bayer SA, Altman J. 1990. Development of layer I and the subplate in the rat neocortex. Exp Neurol. 107:48–62.

Bayer SA, Altman J. 1991. Neocortical development. New York: Raven.

Beaulieu C, Colonnier M. 1989. Number and size of neurons and synapses in the motor cortex of cats raised in different environmental complexities. J Comp Neurol. 289:178–187.

Benes FM, Lange N. 2001. Two-dimensional versus three-dimensional cell counting: a practical perspective. Trends Neurosci. 24:11–17.

Bininda-Emonds OR, Cardillo M, Jones KE, MacPhee RD, Beck RM, Grenyer R, Price SA, Vos RA, Gittleman JL, Purvis A. 2007. The delayed rise of present-day mammals. Nature. 446:507–512.

Blanga-Kanfi S, Miranda H, Penn O, Pupko T, DeBry RW, Huchon D. 2009. Rodent phylogeny revised: analysis of six nuclear genes from all major rodent clades. BMC Evol Biol. 9:71. doi: 10.1186/1471-2148-9-71.

Cahalane DJ, Charvet CJ, Finlay BL. 2012. Systematic, balancing gradients in neuron density and number across the primate isocortex. Front Neuroanat. 6:28. doi: 10.3389/fnana.2012.00028.

Cahalane DJ, Clancy B, Kingsbury MA, Graf E, Sporns O, Finlay BL. 2011. Network structure implied by initial axon outgrowth in rodent cortex: empirical measurement and models. PLoS One. 6:16113. doi:10.1371/journal.pone.0016113.

Campi KL, Collins CE, Todd WD, Kaas J, Krubitzer L. 2011. Comparison of area 17 cellular composition in laboratory and wild-caught rats including diurnal and nocturnal species. Brain Behav Evol. 77:116–130. doi: 10.1159/000324862.

Carlo CN, Stevens CF. 2013. Structural uniformity of neocortex, revisited. Proc Natl Acad Sci USA. 110:1488–1493. doi: 10.1073/pnas.1221398110.

Caviness VS, Nowakowski RS, Bhide PG. 2009. Neocortical neurogenesis: morphogenetic gradients and beyond. Trends Neurosci. 32:443–450.

Chalfin BP, Cheung DT, Muniz JAPC, de Lima Silveira LC, Finlay BL. 2007. Scaling of neuron number and volume of the pulvinar complex in new world primates: comparisons with humans, other primates, and mammals. J Comp Neurol. 504:265–274.

Charvet CJ, Striedter GF. 2011. Developmental modes and developmental mechanisms can channel brain evolution. Front Neuroanat. 5:4. doi: 10.3389/fnana.2011.00004.

Charvet CJ, Striedter GF. 2008. Developmental species differences in brain cell cycle rates between northern bobwhite quail (*Colinus virginianus*) and parakeets (*Melopsittacus undulatus*): implications for mosaic brain evolution. Brain Behav Evol. 72:295–306.

Charvet CJ, Striedter GF, Finlay BL. 2011. Evo-devo and brain scaling: candidate developmental mechanisms for variation and constancy in vertebrate brain evolution. Brain Behav Evol. 78:248–257. doi: 10.1159/000329851.

Chenn A, Walsh CA. 2002. Regulation of cerebral cortical size by control of cell cycle exit in neural precursors. Science. 297:365–369.

Christensen JR, Larsen KB, Lisanby SH, Scalia J, Arango V, Dwork AJ, Pakkenberg B. 2007. Neocortical and hippocampal neuron and glial cell numbers in the rhesus monkey. Anat Rec. 290:330–340.

Clancy B, Darlington RB, Finlay BL. 2001. Translating developmental time across mammalian species. Neuroscience. 105:7–17.

Collins CE. 2011. Variability in neuron densities across the cortical sheet in primates. Brain Behav Evol. 78:37–50.

Collins CE, Airey DC, Young NA, Leitch DB, Kaas JH. 2010. Neuron densities vary across and within cortical areas in primates. Proc Natl Acad Sci USA. 107:15927–15932.

Collins CE, Leitch DB, Wong P, Kaas JH, Herculano-Houzel S. 2013. Faster scaling of visual neurons in cortical areas relative to subcortical structures in non-human primate brains. Brain Struct Funct. 218:805–816.

Dehay C, Giroud P, Berland M, Smart I, Kennedy H. 1993. Modulation of the cell cycle contributes to the parcellation of the primate visual cortex. Nature. 366:464–466.

Dyer MA, Martins R, da Silva Filho M, Muniz JA, Silveira LC, Cepko CL, Finlay BL. 2009. Developmental sources of conservation and variation in the evolution of the primate eye. Proc Natl Acad Sci USA. 106:8963–8968. doi: 10.1073/pnas.0901484106.

Finlay BL. 1992. Cell death and the creation of regional differences in neuronal numbers. J Neurobiol. 23:1159–1171.

Finlay BL, Darlington RB. 1995. Linked regularities in the development and evolution of mammalian brains. Science. 268:1578–1584.

Finlay BL, Hersman MN, Darlington RB. 1998. Patterns of vertebrate neurogenesis and the paths of vertebrate evolution. Brain Behav Evol. 52:232–242.

Finlay BL, Slattery M. 1983. Local differences in the amount of early cell death in neocortex predict adult local specializations. Science. 219:1349–1351.

Friede RL. 1963. The relationship of body size, nerve cell size, axon length, and glial density in the cerebellum. Proc Natl Acad Sci USA. 49:187–193.

Gabi M, Collins CE, Wong P, Torres LB, Kaas JH, Herculano-Houzel S. 2010. Cellular scaling rules for the brains of an extended number of primate species. Brain Behav Evol. 76:32–44. doi: 10.1073/pnas.0901484106.

Giannaris EL, Rosene DL. 2012. A stereological study of the numbers of neurons and glia in the primary visual cortex across the lifespan of male and female rhesus monkeys. J Comp Neurol. 520: 3492–3508.

Hanken J, Wake DB. 1993. Miniaturization of body size: organismal consequences and evolutionary significance. Annu Rev Ecol Syst. 24:501–519.

Herculano-Houzel S, Collins CE, Wong P, Kaas JH. 2007. Cellular scaling rules for primate brains. Proc Natl Acad Sci USA. 104:3562–3567.

Herculano-Houzel S, Lent R. 2005. Isotropic fractionator: a simple, rapid method for the quantification of total cell and neuron numbers in the brain. J Neurosci. 25:2518–2521.

Herculano-Houzel S, Ribeiro P, Campos L, Valotta da Silva A, Torres LB, Catania KC, Kaas JH. 2011. Updated neuronal scaling rules for the brains of Glires (rodents/lagomorphs). Brain Behav Evol. 78:302–314. doi: 10.1073/pnas.0901484106.

Hutsler J, Lee D, Porter K. 2005. Comparative analysis of cortical layering and supragranular layer enlargement in rodent carnivore and primate species. Brain Res. 1052:71–81.

Kaiser M, Hilgetag CC. 2006. Nonoptimal component placement, but short processing paths, due to long-distance projections in neural systems. PLoS Comput Biol. 2:95. doi: 10.1073/pnas.0901484106.

Kaskan PM, Franco ECS, Yamada ES, de Lima Silveira LC, Darlington RB, Finlay BL. 2005. Peripheral variability and central constancy in mammalian visual system evolution. Proc Biol Sci. 272:91–100.

Kennedy H, Dehay C. 1993. Cortical specification of mice and men. Cereb Cortex. 3:171–186.

Klyachko VA, Stevens CF. 2003. Connectivity optimization and the positioning of cortical areas. Proc Natl Acad Sci USA. 100: 7937–7941.

Lent R, Hedin-Pereira C, Menezes JR, Jhaveri S. 1990. Neurogenesis and development of callosal and intracortical connections in the hamster. Neuroscience. 38:21–37.

Lewitus E, Hof PR, Sherwood CC. 2012. Phylogenetic comparison of neuron and glia densities in the primary visual cortex and hippocampus of carnivores and primates. Evolution. 66:2551–2563. doi: 10.1073/pnas.0901484106.

Lidow MS, Song Z-M. 2001. Primates exposed to cocaine in utero display reduced density and number of cerebral cortical neurons. J Comp Neurol. 435:263–275. doi: 10.1073/pnas.0901484106.

McGowan LD, Alaama RA, Freise AC, Huang JC, Charvet CJ, Striedter GF. 2012. Expansion, folding, and abnormal lamination of the chick optic tectum after intraventricular injections of FGF2. Proc Natl Acad Sci USA. 109:10640–10646.

Miyama S, Takahashi T, Nowakowski RS, Caviness VS Jr. 1997. A gradient in the duration of the G1 phase in the murine neocortical proliferative epithelium. Cereb Cortex. 7:678–689.

Modha DS, Singh R. 2010. Network architecture of the long-distance pathways in the macaque brain. Proc Natl Acad Sci USA. 107:13485–13490.

Murphy WJ, Eizirik E, Johnson WE, Zhang YP, Ryder OA, O'Brien SJ. 2001. Molecular phylogenetics and the origins of placental mammals. Nature. 409:614–618.

Murre JMJ, Sturdy DPF. 1995. The connectivity of the brain: multi-level quantitative analysis. Biol Cybern. 73:529–545.

O'Kusky J, Colonnier M. 1982. A laminar analysis of the number of neurons, glia, and synapses in the adult cortex (area 17) of adult macaque monkeys. J Comp Neurol. 210:278–290.

Rakic P. 2008. Confusing cortical columns. Proc Natl Acad Sci USA. 105:12099–12100.

Rakic P. 2009. Evolution of the neocortex: a perspective from developmental biology. Nat Rev Neurosci. 10:724–735.

Rakic P. 1974. Neurons in rhesus monkey visual cortex: systematic relation between time of origin and eventual disposition. Science. 183:425–427.

Rakic P. 2002. Pre- and post-developmental neurogenesis in primates. Clin Neurosci Res. 2:29–39.

Reep RL, Finlay BL, Darlington RB. 2007. The limbic system in mammalian brain evolution. Brain Behav Evol. 70:57–70.

Rockel AJ, Hiorns RW, Powell TPS. 1980. The basic uniformity in structure of the neocortex. Brain. 103:221–244.

Sherwood CC, Raghanti MA, Stimpson CD, Bonar CJ, de Sousa AA, Preuss TM, Hof PR. 2007. Scaling of inhibitory interneurons in areas v1 and v2 of anthropoid primates as revealed by calcium-binding protein immunohistochemistry. Brain Behav Evol. 69:176–195.

Smart IH. 1983. Three dimensional growth of the mouse isocortex. J Anat. 137:683–694.

Stephan H, Frahm H, Baron G. 1981. New and revised data on volumes of brain structures on insectivores and primates. Folia Primatol (Basel). 35:1–29.

Striedter GF. 2005. Principles of brain evolution. Sunderland (MA): Sinauer.

Striedter GF, Charvet CJ. 2008. Developmental origins of species differences in telencephalon and tectum size: morphometric comparisons between a parakeet (*Melopsittacus undulatus*) and a quail (*Colinus virgianus*). J Comp Neurol. 507:1663–1675. doi: 10.1002/cne.21640.

Suner I, Rakic P. 1996. Numerical relationship between neurons in the lateral geniculate nucleus and primary visual cortex in macaque monkeys. Vis Neurosci. 13:585–590.

Suter B, Nowakowski RS, Bhide PG, Caviness VS. 2007. Navigating neocortical neurogenesis and neuronal specification: a positional information system encoded by neurogenetic gradients. J Neurosci. 27:0777–10784.

Watts DJ, Strogatz SH. 1998. Collective dynamics of 'small-world' networks. Nature. 393:440–442.

Williams RW, Rakic P. 1988. Three-dimensional counting: an accurate and direct method to estimate numbers of cells in sectioned material. J Comp Neurol. 278:344–352.

Williams RW, von Bartheld CS, Rosen GD. 2003. Counting cells in sectioned material: a suite of techniques, tools, and tips. Curr Protoc Neurosci. 1.11.1–1.11.29. doi: 10.1002/cne.21640.

Workman AD, Charvet CJ, Clancy B, Darlington RB, Finlay BL. 2013. Modeling transformations of neurodevelopmental sequences across mammalian species. J Neurosci. 33:7368–7383. doi: 10.1523/JNEUROSCI.5746-12.2013.

Young NA, Collins CE, Kaas JH. 2013. Cell and neuron densities in the primary motor cortex of primates. Front Neural Circuits. 7:30. doi:10.3389/fncir.2013.00030.